# A Detailed Kinetico-Mechanistic Investigation on the Palladium C–H Bond Activation in Azobenzenes and their Monopalladated Derivatives

Alen Bjelopetrović,[a‡] Dajana Barišić,[a‡] Zrinka Duvnjak,[b] Ivan Džajić,[b] Marina Juribašić Kulcsar,[a] Ivan Halasz,[a] Manuel Martínez,[c,d*] Ana Budimir,[b*] Darko Babić,[a*] and Manda Ćurić,[a*]

[a]Ruđer Bošković Institute, Division of Physical Chemistry, Bijenička 54, HR-10000 Zagreb, Croatia

[b]Faculty of Pharmacy and Biochemistry, University of Zagreb, Ante Kovačića 1, 10000 Zagreb, Croatia

[c]Departament de Química Inorgànica i Orgànica, Secció de Química Inorgànica, Martí i Franquès 1-11, E-08028 Barcelona, Spain

[d]Institute of Nanoscience and Nanotechnology (IN2UB), Universitat de Barcelona, Barcelona, Spain

*Supporting Information Placeholder*

**ABSTRACT:** Palladium C–H bond activation in azobenzenes with $R_1$ and $R_2$ at *para*-positions of the phenyl rings ($R_1$=N(Me)$_2$, $R_2$=H (**L1**); $R_1$=N(Me)$_2$, $R_2$=Cl (**L2**); $R_1$=N(Me)$_2$, $R_2$=I (**L3**); $R_1$=–N(Me)$_2$, $R_2$=NO$_2$ (**L4**); $R_1$=H, $R_2$=H (**L5**)) and their already monopalladated derivatives, using *cis*-[PdCl$_2$(DMF)$_2$] as precursor, has been studied in detail by *in situ* $^1$H NMR spectroscopy in *N,N*-dimethylformamide-$d_7$ (DMF-$d_7$) at room temperature; the same processes have been monitored in parallel via time-resolved UV-Vis spectroscopy in DMF at different temperatures and pressures. The final goal being to achieve, from a kinetico-mechanistic perspective, a complete insight of previously reported reactivity results. As expected, the results suggest the operation of an electrophilic substitution intimate mechanism for both the mono- and dipalladation reactions, occurring from the coordination compound and the monopalladated intermediates, respectively. The process involves a deprotonation of the C–H bond, which is assisted by the presence of a coordinated DMF molecule, that acts as a base. For the first time, NMR monitoring provides a direct evidence of all the intermediate stages, that is: *i)* coordination of the azo ligand to a Pd$^{II}$ center, *ii)* formation of the monopalladated species, *iii)* coordination of the monopalladated species to another Pd$^{II}$ unit, which finally result in the *iv)* formation of the dipalladated product. All of these species have been identified as intermediates in the dipalladation of azobenzenes, evidenced also by UV-Vis spectroscopy time-resolved monitoring; the data also confirms that the cyclopalladation of asymmetrically substituted azobenzenes occurs by two concurrent reaction paths. In order to identify the species observed by NMR and by UV-Vis spectroscopies, the final products, intermediates and the Pd$^{II}$ precursor have been prepared and characterized by X-ray diffraction, IR and NMR spectroscopies. All attempts to isolate the intermediate monopalladated complexes attached to another Pd$^{II}$ unit proved to be unsuccessful. DFT calculations have also been used in order to explain the isomerism observed for the isolated complexes, as well as to assign their NMR spectra.

## INTRODUCTION

Cyclopalladation continuously attracts considerable interest not only as the most direct route for the synthesis of palladacycles[1] but also as a generally important reaction in organic synthetic chemistry.[2] Palladacycles are identified as crucial intermediates in many organic reactions promoted by palladium precursors, that result in functionalized hydrocarbons.[1,2] Therefore, a detailed understanding of cyclopalladation pathways of different organic substrates is essential. Cyclopalladation is recognized as a two-step reaction involving the coordination of palladium center by a directing group, which leads to selective intramolecular activation of the C–H bond, resulting in the formation of the Pd–C bond with a simultaneous release of proton and ring closure.[1c,3] This mechanism is supported by our kinetico-mechanistic studies on a variety of compounds,[4] and specifically with our previously published studies on the mono- and dicyclopalladation of azobenzene and its 4,4'-functionalized derivatives using *trans*-[PdCl$_2$(MeCN)$_2$] as a precursor.[4b]

The kinetics of the latter processes had been studied by UV-Vis time-resolved spectroscopy in *N,N*-dimethylformamide (DMF) as solvent at room temperature, as this is the solvent for numerous Pd$^{II}$-catalyzed reactions.[2f,5] The linear free energy correlations of the experimental kinetic data with the DFT calculations, provided again a convincing mechanistic picture of the electrophilic attack at the phenyl ring within the Pd-azobenzene complex.[4a,b]

As a natural extension for the complete understanding of that work, here we present the comprehensive kinetico-mechanistic study of the cyclopalladation of azobenzenes and their monopalladated compounds (Scheme 1) by UV-Vis spectroscopy. The parallel, time-resolved, $^1$H NMR study has allowed, for the first time, a full and detailed insight into the nature and reactivity of the intermediates formed during these reactions. The structure of most of these NMR spectroscopy observed intermediates, as well as of the $Pd^{II}$ precursor, *cis*-[$PdCl_2(DMF)_2$], have been isolated and characterized both structurally and spectroscopically. The UV-Vis spectroscopy study at different temperatures and pressures has allowed for the first time the obtention of detailed kinetico-mechanistic information by determining activation parameters, both thermal ($\Delta H^{\ddagger}$, $\Delta S^{\ddagger}$) and pressure ($\Delta V^{\ddagger}$).

**Scheme 1. Molecular structure of the azobenzenes, and their coordination, mono- and dicyclopalladated derivatives, used in this study. Only α-isomers of An, Mn and MAn are shown**

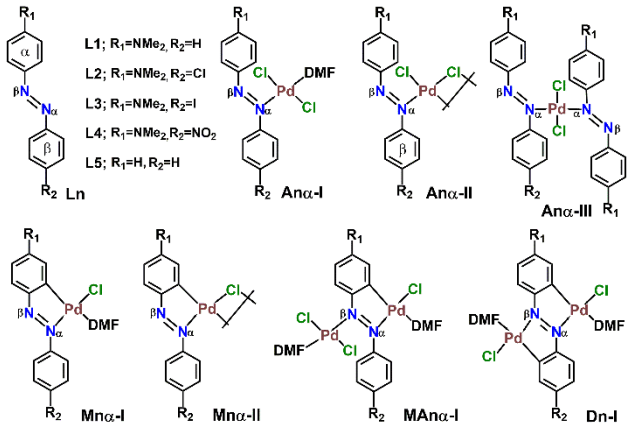


## RESULTS AND DISCUSSION

**Compounds.** The $Pd^{II}$ precursor, coordination, mono-and dipalladated complexes of azobenzenes (Scheme 1) have been isolated and structurally characterized by X-ray diffraction and IR spectroscopy in the solid-state, and by NMR spectroscopy in solution.

**$Pd^{II}$ precursor**. The *cis*-[$PdCl_2(DMF)_2$] was obtained in high yield by aging $PdCl_2$ in a vapor of *N,N*–dimethylformamide (DMF).[6] Its molecular structure, resolved by powder X-ray diffraction (PXRD), indicates a *cis*-configuration and the coordination of the oxygen atoms of the two DMF ligands to the $Pd^{II}$ center (Figure 1). Despite existing reports on the isolation and characterization of the *trans*-isomer of this precursor, all attempts to obtain pure either *cis*- or *trans*-[$PdCl_2(DMF)_2$] from DMF solutions were unsuccessful.[7] Evidently, although under our conditions the [$PdCl_2(DMF)_2$] complex was isolated in the *cis*-form, an equilibrium between *cis*- and *trans*-isomers in DMF solution cannot be ruled out. DFT calculations support this finding; only a small 1 kcal/mol difference, favoring the *cis*-[$PdCl_2(DMF)_2$] isomer, exists between the free energies of the two possible configurations in DMF solution.[4b]

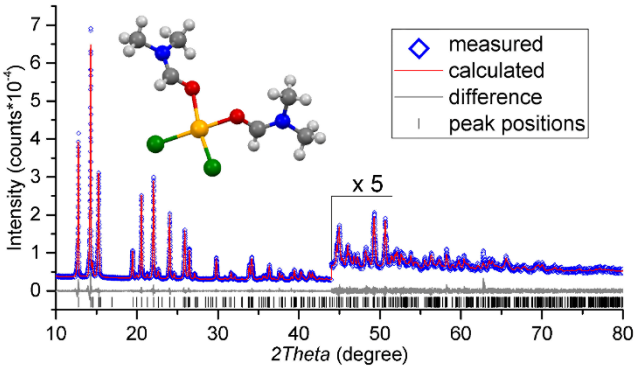


**Figure 1**. Powder X-ray diffraction of the calculated molecular structure of *cis*-[$PdCl_2(DMF)_2$] and its final Rietveld refinement.

**Coordination compounds (Anα)**. The coordination compounds of the azobenzenes studied with $PdCl_2$ were prepared as acetonitrile derivatives in acetonitrile solution. According to the procedure developed by our group, compound **A2α-I** has been prepared and characterized before.[8] The reactions of 4-(*N,N*-dimethylamino)azobenzene (**L1**), 4-(*N,N*-dimethylamino)-4'-chloroazobenzene (**L2**) and 4-(*N,N*-dimethylamino)-4'-iodoazobenzene (**L3**) with $PdCl_2$ in a 1:1 molar ratio (**Ln** to Pd) afforded single crystals of the respective acetonitrile derivatives of **A1α-I**, **A2α-I** and **A3α-I** complexes (Figures 2, S3 and S4). Despite the fact that two isomers, α and β, can be formed in the reactions of $PdCl_2$ with the unsymmetrically substituted azobenzenes (due to similar coordination abilities of two azo-nitrogens, $N_\alpha$ and $N_\beta$),[9] all the coordination compounds obtained show the palladium center bound to the $N_\alpha$ donor of azobenzene, an acetonitrile, and two chlorides in *trans* positions. The $^1$H NMR spectra of the compounds indicated that their structures in $CD_3CN$ solution are consistent with those observed in the solid state. The spectra contain only one set of signals, assigned to the α isomers indicated in Scheme 1. Coordination of the palladium center to the $N_\alpha$ donor produces a large downfield shift of *ortho* protons H-2,6 and H-8,12 (see Scheme S1 for numbering) signals relative to the free ligand (see Experimental and Tables S4-S8); these appear now in the 8.0 to 10.0 ppm region, characteristic for the coordination complexes of azobenzenes.[8] The formation of the DMF **Anα-I** compounds indicated in Scheme 1 is attained on dissolving the acetonitrile derivatives of the **Anα-I** structure in DMF, as evidenced by the NMR spectra (see Tables S4-S8).

Although for these **L1**, **L2** and **L3** azobenzene derivatives only monomeric species have been detected, for 4-

(*N,N*-dimethylamino)-4'-nitroazobenzene (**L4**) a mixture of monomeric and dimeric coordination compounds (**A4α-I** and **A4α-II**, Scheme 1) were obtained, all attempts to isolate pure monomeric or dimeric species derived from **L4** proved unsuccessful. Contrary to that observed for the unsymmetrical **L1-L4** systems, regardless of the reactants' to Pd molar ratio used, reaction of **L5** with $PdCl_2$ yielded exclusively the already prepared and characterized[10] *bis*-complex **A5α-III** (Scheme 1) having two azobenzenes attached to the palladium center. The product was structurally identified in the solid state by comparison of its powder diffraction (PXRD) pattern with that simulated from its known single crystal structure (Figure S1).[10]

**Monopalladated azobenzene complexes (Mnα-I, Mnα-II)**. Stirring in DMF solution of the isolated coordination complexes indicated above afforded the monopalladated monomeric **M1α-I – M3α-I**, or dimeric **M4α-II** compounds, (Scheme 1). The analogous reaction with **A5-III** resulted in a mixture of free azobenzene ligand, monopalladated and dipalladated species. Neat **M5-II**, was only obtained by the reaction of **L5** and $Na_2[PdCl_4]$ in methanol solution, as already described.[11] The $^1$H NMR spectral data, along with the elemental analysis (see Experimental), support the formulations of the isolated monopalladated products as monomeric [PdCl(Ln–H)(DMF)] (**M1α-I**, **M2α-I**, and **M3α-I**) and dimeric $[Pd(\mu\text{-}Cl)(Ln–H)]_2$ (**M4α-II** and **M5-II**) species. X-ray single-crystal diffraction analysis of the new monomeric **M1α-I** and known[8] **M2α-I** products confirmed the formation of the isomer with the palladium center bonded to $N_\alpha$ and to the phenyl ring bearing the electron-donating $NMe_2$ group (Figures 2, S5 and Table S1). In both complexes, the metal center is additionally bonded to a chloride and a DMF (O-donor) *trans* to the $Pd^{II}$–C bond. Corroboration for the formation of dimeric monopalladated azobenzene **M5α-II** was obtained from its powder diffraction (PXRD) pattern, which is in good agreement with that simulated from the already known single crystal structure[12] (Figure S2). $^1$H NMR spectra of the dimeric **M4α-II** and **M5-II** compounds indicate that these convert into the monomeric **M4α-I** and **M5-I** in DMF solution; the NMR shift pattern of their signals being equivalent to those found for the isolated monomeric **M1α-I – M3α-I** compounds.

**Monopalladated-palladium coordinated complexes (MAnα)**. All attempts to prepare these species (Scheme 1) following the same procedure used for the preparation of the coordination complexes of **Anα**-type, i.e. the reactions of *cis*-$[PdCl_2(DMF)_2]$ and the monopalladated complexes **Mnα** in acetonitrile proved unsuccessful.

**Dipalladated azobenzenes (Dn-I).** The known dipalladated **D1-I – D5-I** (Scheme 1) compounds were prepared in DMF solution by the reaction of monopalladated products **M1α-I – M3α-I, M4α-II, M5-II** with *cis*-$[PdCl_2(DMF)_2]$. As already described,[4b,13] the use of two equivalents of palladium precursor per free palladation sites is needed to avoid the blocking of the precursor by chloride release.

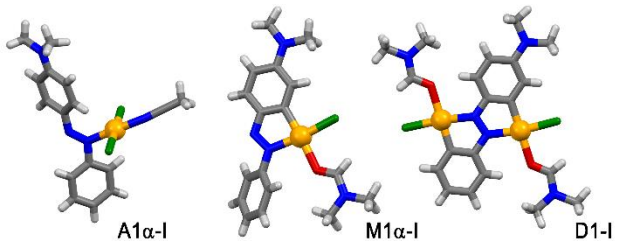


**Figure 2**. Determined molecular structures of **A1α-I** (as acetonitrile derivative), **M1α-I** and **D1-I**.

The products were structurally identified by comparison with the PXRD, IR and NMR spectra of the already known compounds. Additionally, single crystals were also obtained and analyzed for **D1-I** (Figure S6, Table S1); bond distances and angles around the palladium coordination sphere are similar to those found and calculated for other dipalladated azobenzenes.[4b,13] IR spectra agrees with presence of DMF molecules acting as O-donor ligands in **Dn-I** and **Mnα-I** complexes.

**DFT calculations on the speciation of the compounds studied**. The different isomeric forms of the isolated coordination and monopalladated complexes prompted us to carry out some DFT calculations to explain the speciation observed in the reaction medium. The equilibrium constants between **Anα-I**, **Anα-II** and **Anα-III**, as well as between **Mnα-I** and **Mnα-II**, were evaluated from the quantum-chemical Gibbs energies of the corresponding molecular species. The predicted equilibrium compositions at experimental concentrations involved only **Anα-I** and **Anα-III** species. While **A1α-I** and **A5α-III** were predicted as major forms, in agreement with experimental findings, **A2α-III** and **A3α-III** were expected as dominant, in contrast with the fact that only **A2α-I** and **A3α-I** have been isolated. This deviation is, nevertheless, within the (in)accuracy of the computational modelling. All **Anα-II** complexes were predicted to be at a negligible concentration level, which is again in contrast with the isolation of a mixture of **A4α-I** and **A4α-II**. All monopalladated monomeric species, **Mnα-I**, were expected as dominant, in opposition to the experimentally observed **M4α-II** single component reaction mixture; for the **L4** ligand, the presence of the $-NO_2$ substituent probably involves some specific solvent interactions that are beyond the modelling capabilities.

**Kinetico-mechanistic studies**. Our previous UV-Vis monitoring of the reactions at 25 °C and atmospheric pressure had indicated that the dipalladation of the azobenzenes used in this study is a multistep process. The full reactivity involves the formation of the intermediates **Anα-I** and **MAnα-I** (see Scheme 1) in fast pre-equilibria, prior to the rate-determining steps generating mono- and dipalladated species **Mnα-I** and **Dn-I**, respectively, (Scheme 2 and equations (1) and (2)).[4b]

**UV-Vis time-resolved monitoring**. Since the full set of activation parameters, $\Delta H^{\ddagger}$, $\Delta S^{\ddagger}$ and $\Delta V^{\ddagger}$, provide determinant information on the cyclopalladation mechanism,[4e,15] the reactions of **L1-L4** and **M1α-I – M4α-I**, with *cis*-$[PdCl_2(DMF)_2]$ in DMF were monitored by UV-

Vis time-resolved spectroscopy at varying temperatures and pressures.

**Scheme 2. Full dipalladation process of the azobenzenes studied.[4b] {Pd} represents *cis*-[Pd(Cl$_2$(DMF)$_2$].**

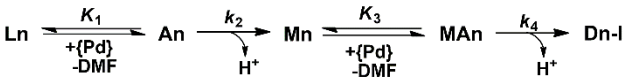


$$k_{obs(1)} = \frac{k_2 K_1 [PdCl_2(DMF)_2]}{1+K_1[PdCl_2(DMF)_2]} \quad (1)$$

$$k_{obs(2)} = \frac{k_4 K_3 [PdCl_2(DMF)_2]}{1+K_3[PdCl_2(DMF)_2]} \quad (2)$$

All reactions were carried out under pseudo-first order conditions, with a large molar excess of the palladium coordination complex precursor. The monitoring of the reactions of **L1-L4** with *cis*-[PdCl$_2$(DMF)$_2$] indicated the presence of two rate-determining steps in the full palladation process, as observed before. The observed pseudo-first order constants $k_{obs(1)}$ and $k_{obs(2)}$ were calculated from the time-resolved spectral changes using a consecutive A →B →C model. The dependence of $k_{obs(1)}$ and $k_{obs(2)}$ on the *cis*-[PdCl$_2$(DMF)$_2$] (in excess, Figure 3) concentration, and previously published work,[4b] lead us to consider as valid the reaction mechanism and rate law depicted by Scheme 2 and equations (1) and (2) for the systems studied. The lack of curvature in the plots of Figure 3 indicate that $K_1$ and $K_3$ have low enough values to avoid a saturation behaviour.[15] The values of the $k_2K_1$ and $k_4K_3$ products for the reactions of the **L1-L4** ligands, determined from the slopes of the $k_{obs(1)}$ and $k_{obs(2)}$ versus [Pd] data at variable temperature and pressure (Table S2, Figures 3 and S7), agree with former experiments at room temperature.[4b]

It is noticeable that, as shown in Figure 4, the time-resolved spectral changes recorded during the reaction of *cis*-[PdCl$_2$(DMF)$_2$] with the prepared monometallated complexes **M1α-I – M4α-I** can be fitted to the simple A →B model. The set of pseudo-first-order rate constants $k_{obs}$ derived show a linear dependence on the palladium concentration (Figure S8), and produce a set of second order rate constants, $k_4K_3$, (Table S2), that are expected to be equivalent to that obtained for the second part of the mechanism in Scheme 2, i.e., the second cyclopalladation of **Ln**.[4b]

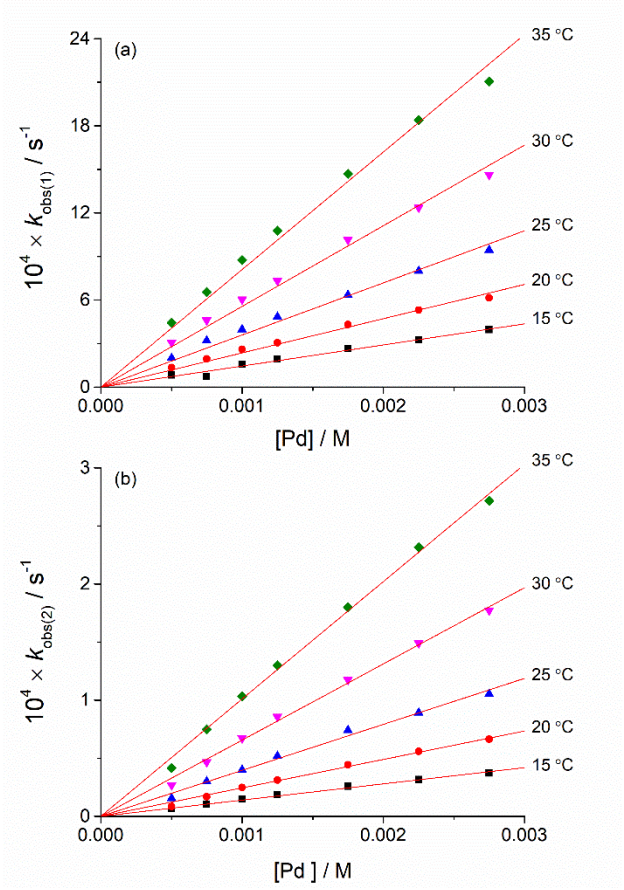


**Figure 3**. Dependence of the pseudo-first-order rate constants for the first, $k_{obs(1)}$, (a) and second, $k_{obs(2)}$, (b) cyclopalladation of **L2** on the [Pd] concentration in DMF at different temperatures;[**L2**] = 25 μM.

Interestingly, the actual values of $k_4K_3$ measured from the **M1α-I – M4α-I** complexes are definitively diverse from those obtained when the reaction was monitored as the second step of the reaction between the palladium precursor and the **L1-L4** azo ligands (see Figure 5a). The only way to explain this difference is by accepting the existence of a concurrent reaction scheme involving two different cyclopalladation processes, i.e. on both the preparatively isolated **Anα-I** compounds and the putative **Anβ-I** undetected isomer of the initial coordination complexes (Scheme 3).

The fitting of the variation of $k_2K_1$ and $k_4K_3$ for the reaction of **Ln**, or $k_4K_3$ for that of **M1α -I**, with the *cis*-[PdCl$_2$(DMF)$_2$] precursor at different temperatures using the standard Eyring plots (Figures 5a and S9), produce the values of the thermal activation parameters ($\Delta H^{\ddagger}$ and $\Delta S^{\ddagger}$) indicated in Table 1.

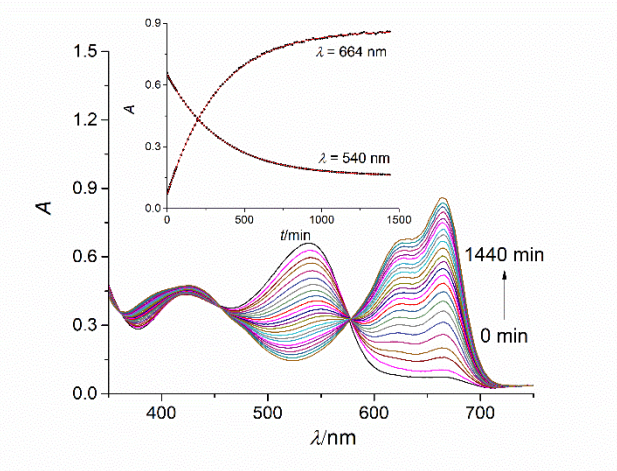


**Figure 4**. UV-Vis time-resolved spectral changes for the reaction of *cis*-[$PdCl_2(DMF)_2$] in DMF solution with **M2α-I**. [**M2α**] = 25 μM, [Pd] = 1.0 mM, T = 25 °C Inset shows the kinetic traces at 540 and 664 nm, along with their fitting to an A → B process.

In the same manner, the pressure activation parameters ($\Delta V^{\ddagger}$), determined by the variation of the second order rate constants for the reaction of **Ln** with the palladium precursor (calculated as $k_{obs}$/[Pd], see Experimental) at different pressures using the standard ln($k$) versus $P$ equation (Figures 5b and S10), are also summarized in Table 1.

**Table 1. Summary of the kinetic (298 K) and thermal and pressure activation parameters determined for the cyclopalladation reaction of azobenzenes L1-L4 and their monopalladated derivatives M1α-I - M4α-I in DMF.**

| Compound | $^{298}k_2K_1$ $M^{-1}$ $s^{-1}$ | $\Delta H_1^{\ddagger}$ kJ $mol^{-1}$ | $\Delta S_1^{\ddagger}$ $JK^{-1}$ $mol^{-1}$ | $\Delta V_1^{\ddagger}$ $cm^3$ $mol^{-1}$ | $^{298}k_4K_3$ $M^{-1}$ $s^{-1}$ | $\Delta H_2^{\ddagger}$ kJ $mol^{-1}$ | $\Delta S_2^{\ddagger}$ J $K^{-1}$ $mol^{-1}$ | $\Delta V_2^{\ddagger}$ $cm^3$ $mol^{-1}$ |
|---|---|---|---|---|---|---|---|---|
| **L1** | 0.44 | 64 ± 2 | −37 ± 6 | −12 ± 1 | 0.060 | 60 ± 3 | −67 ± 8 | −15 ± 2 |
| **M1α-I** | – | – | – | – | 0.071 | 59 ± 1 | −71 ± 2 | |
| **L2** | 0.39 | 62 ± 2 | −47 ± 6 | −11 ± 2 | 0.040 | 70 ± 1 | −36 ± 3 | −8± 1 |
| **M2α-I** | – | – | – | – | 0.046 | 63 ± 2 | −60 ± 6 | |
| **L3** | 0.40 | 57 ± 2 | −62 ± 7 | −11 ± 2 | 0.055 | 64 ± 1 | −52 ± 3 | −12 ± 2 |
| **M3α-I** | | | | | 0.067 | 62 ± 1 | −59 ± 3 | |
| **L4** | 0.25 | 63 ± 1 | -47 ± 3 | -8.3 ± 0.1 | 0.030 | 66 ± 3 | -50 ± 8 | -8 ± 1 |
| **M4α-I** | — | — | — | – | 0.038 | 64 ± 1 | −62 ± 4 | |

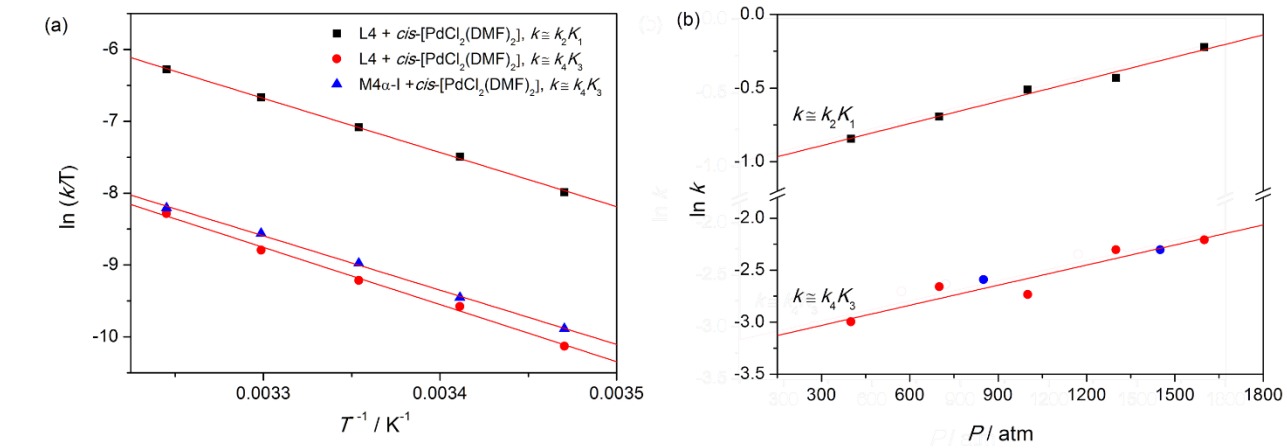


**Figure 5.** a) Eyring plots for the cyclopalladation reactions of **L4** and **M4α–I**. b) ln $k$ versus $P$ plot for the cyclopalladation reactions of **L1** and **M1α**–I (blue circles).

The pressure variation of the values of $k_4K_3$ for the reaction leading to **D1-I** using the **M1α-I** intermediate with *cis*-[$PdCl_2(DMF)_2$], instead of the starting **L1** azobenzene, was also conducted at 850 and 1450 atm. As seen in Figures 5b and S10, the values determined are in very close agreement with those obtained for the second step observed on the reaction of the precursor with of **L1**. We presumed an equivalent (within error) behavior for all **Mnα-I** derivatives, and further high-pressure experiments of the reactions of **Mnα-I** were not conducted. So, $\Delta V_2^{\ddagger}$ was considered independent of the origin of the monometallated intermediate within the error involved in its determination.

The interpretation of the values of the activation parameters obtained, and summarized in Table 1, is not straightforward in several ways. To start with, the values cannot be assigned to a simple kinetic step, as the determined rate constants are composites of an equilibrium constant for the formation of intermediates **Anα-I** or **MAnα-I** and the first-order rate constant for the subsequent C–H bond activation (Scheme 2 and equations 1 and 2). Therefore, the thermal and the pressure activation parameters correspond to this product, and include the values of $\Delta H^{\circ}$, $\Delta S^{\circ}$, and $\Delta V^{\circ}$ for the formation equilibrium constants ($K_1$ and $K_3$). Even more, only the values corresponding to the palladation from compounds **Mnα-I** correspond to a proper single reaction pathway. For all the other processes studied, the reactivity could correspond to that of a mixture of the α and the putative β isomer of **An-I** and **Mn-I** complexes (see above, next section and Scheme 1). This is evident from the values of $\Delta H_2^{\ddagger}$ and $\Delta S_2^{\ddagger}$ collected in Table 1 for the dipalladation of the **Ln** derivatives, that should correspond to the average of the reaction occurring on the α (determined as indicated) and β isomers of **Mn-I**.

Interestingly, comparison of the data observed for the second palladation processes indicates that the values expected for the reactions occurring on the α unit of the **Mnβ-I** compounds have larger activation enthalpies and less negative activation entropies, in order to attain the average data obtained as the second palladation of **Ln**. It seems clear that the metalation of the β-monometalated complexes with the palladium attached to the $N_\alpha$ donor, **MAnβ-I**, has an earlier transition state with lower ordering but with higher enthalpy demands that has to be related to the presence of the donor $-NMe_2$ ($R_1$, see Scheme 1) on the *meta* position of the activating C–H bond.

Even with these difficulties in their final interpretation, plus the fact the DMF-assisted process involves the exit of a positively charged $\{HDMF\}^+$ unit, the values of the activation parameters depicted in Table 1, are within the range of those determined for other C–H bond activations via electrophilic substitution. [3a-3c,4d] The negative values of $\Delta S^{\ddagger}$ and $\Delta V^{\ddagger}$ for both palladation steps agree with the presence of a highly ordered transition state in the rate determining step, which is supported by the computational study of the cyclopalladation mechanism.[3a,-3c,4a,b,d]

**NMR time-resolved monitoring.** Since the presence of coordination intermediates has not been detected by UV-Vis spectroscopy, and the detailed structure of the intermediate species detected cannot be assessed by the technique, time-resolved $^1$H NMR monitoring of the reactions of **Ln** and **Mnα-I** with *cis*-$[PdCl_2(DMF)_2]$ was conducted (Figures S11-S16). The procedure enabled the obtention of the concentration profiles of the species indicated in Scheme 3 (Figures S17-S25) and provided a detailed insight into the reaction dynamics.

**Scheme 3. Kinetic model for the dipalladation of the azobenzenes used with *cis*-$[PdCl_2(DMF)_2]$ precursor (labeled as {Pd}).**

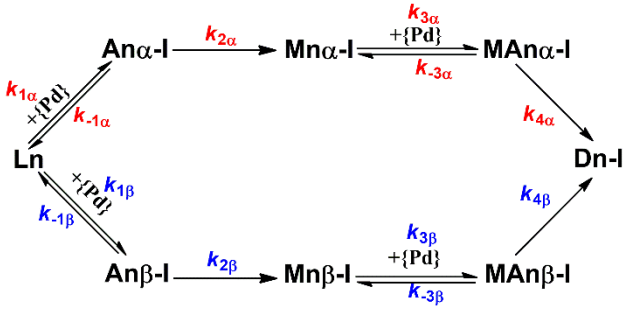


The kinetic model in Scheme 3 assumes two parallel cyclopalladation reaction pathways. These occur on the two possible isomers of the initial coordination compounds, that is **Anα-I** and **Anβ-I**. In both pathways, and for both mono- and di-cyclopalladation steps, the formation of each coordination complex is assumed to be a reversible process, while the subsequent proton transfer is considered as rate determining and irreversible, due to the removal of the aromatic proton. Effectively, the $^1$H NMR spectra of the reaction mixture at different times is consistent with the presence of the species indicated in Scheme 3. The signals of the **Anα-I** species were easily identified from the known spectra of the isolated α-adducts, and those of **Anβ-I** were recognized by their similarity with the α-counterparts (Figure S11).

Confirmation of the formation of both α- and β-isomers was obtained from the reaction **L5** with *cis*-$[PdCl_2(DMF)_2]$, where a single set of signals for **A5-I** was observed, given the equivalence of the $N_\alpha$ and $N_\beta$ donors in **L5** (Figures S13 -S15). The signals of the **Mnβ-I** complexes were assigned based on similarities of their dynamics and NMR shifts, with **Mnα-I** species, and those of **MAnα,** were ascertained from the simpler reactions initiated from **Mnα-I** (Figure S16). The concentrations of **MAnβ** were found, in all cases, too low to be detected or quantified reliably in the NMR spectra.

As indicated in the Experimental section, the NMR time-resolved speciation data was fed into the Dynafit software,[16] with the kinetic model corresponding to Scheme 3. Even though **M4α-I** and **M5-I** were effectively isolated as **M4α-II** and **M5-II**, the formation of the final **Dn-I** complexes always proceed via **Mnα-I** and **Mnβ-I**. Also, although azobenzenes are potentially able to bind to two Pd centers, these species were never detected despite the 10-fold excess of Pd precursor used in the experiments. In this respect, computational results do not provide any reason for such absence,[4b] hence their presence as transient species cannot be ruled out. However, if present in any significant amounts, the species should manifest themselves in the reaction kinetics, a fact that has not been observed.

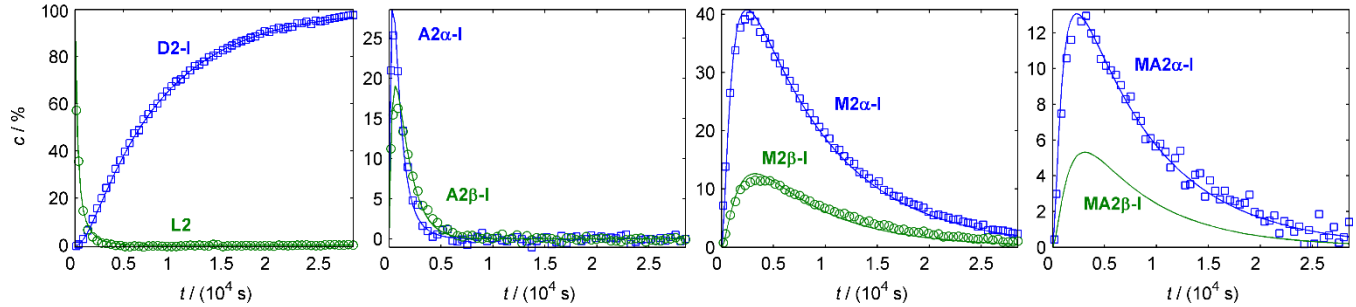


**Figure 6**. Experimental data and fitted concentration profiles for all the species present in the medium for the reaction of **L2** with *cis*-$[PdCl_2(DMF)_2]$. Concentrations are given as percentages of the initial **L2** concentration. No reliable experimental data could be obtained for **MA2β-I**.

Quantitative modelling of NMR experiments by Dynafit software[16] was attempted for all reactions, but only the **L2**/**M2α-I** system produced reliable enough concentration profiles fits for all the species present in the reaction medium. Interestingly, this system is the one showing the largest differences between the data derived from the metallation of the **Mnα-I** compound (starting from the azo ligand or the monometallated derivative), see Table 1, indicating that it is in this reaction where the existence of a β-path is more significant. For the rest of the systems, NMR signal overlapping and poor signal-to-noise ratio did not allow the obtention of of quantitative kinetic traces. Figures 6 and 7, and Table 2 collect the NMR speciation profiles, fitted kinetic traces and the derived second order rate constants for the reaction of full cyclopalladation of **L2**, and that of its monometallated **M2α-I** intermediate, with the *cis*-$[PdCl_2(DMF)_2]$ precursor.

For the reactions from **L1-L4** the concentration profiles indicated always higher concentrations of all α-species, compared with their β-isomers (Figures S17-S20), as expected from the preparative results indicated before. The observed difference can be interpreted as a higher stability (or a faster formation) of the α-isomers; in the case of the **Anα-I** and **Anβ-I** complexes this fact is consistent with the relation between the equilibrium constants ($K_{1\alpha}=k_{1\alpha}/k_{-1\alpha}$) > ($K_{1\beta}=k_{1\beta}/k_{-1\beta}$). Similarly, from the data collected in Table 2 we can assume that the coordination complexes, **Anα-I** or **Anβ-I,** undergo the first C–H bond activation in a slow step, and that the **Mnα-I** species are formed faster than the **Mnβ-I** isomers, as expected for the cyclopalladation occurring preferentially on the ring bearing the electron-donating -$NMe_2$ group (see previous compounds section).[17]

**Table 2. The fitted rate constants for the cyclopalladation of ligand L2 and its monopalladated derivative M2α-I.**

| Rate constants | Compounds | |
|---|---|---|
| | **L2** | **M2α-I** |
| $k_{1\alpha}$ ($M^{-1}s^{-1}$) | 0.43 | – |
| $k_{-1\alpha}$ ($s^{-1}$) | 0.00076 | |
| $k_{1\beta}$ ($M^{-1}s^{-1}$) | 0.191 | – |
| $k_{-1\beta}$ ($s^{-1}$) | 0.00048 | |
| $k_{2\alpha}$ ($s^{-1}$) | 0.0019 | – |
| $k_{2\beta}$ ($s^{-1}$) | 0.00064 | – |
| $k_{3\alpha}$ ($M^{-1}s^{-1}$) | * | 0.56 |
| $k_{-3\alpha}$ ($s^{-1}$) | * | 0.0075 |
| $k_{3\beta}$ ($M^{-1}s^{-1}$) | * | – |
| $k_{-3\beta}$ ($s^{-1}$) | * | |
| $k_{4\alpha}$ ($s^{-1}$) | 0.00053 | 0.000540 |
| $k_{4\beta}$ ($s^{-1}$) | 0.00048 | – |

*Due to significant uncertainty, these rate constants are omitted.

Remarkably, the reaction of intermediate **M5-I** to produce **D5-I** was only completed after one month under NMR concentration conditions, which effectively indicates that mono- and dipalladation processes can be considered as two fully separate processes for this system (Figures S12-S13). For the rest of the systems, the dicyclopalladated products are formed immediately once the monopalladated intermediates are present in the reaction medium (Figure S11). The reaction profiles indicated that the formation rates of mono- or dipalladated species increase in the order **L5** (**M5**) < **L4** (**M4**) < **L2** (**M2**) < **L3** (**M3**) < **L1** (**M1**), which is consistent with the donor strengths of 4,4'-substituents on azobenzenes.

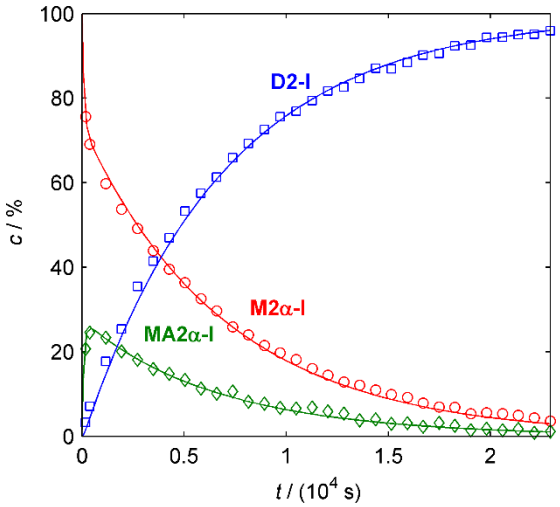


**Figure 7**. Experimental data and fitted concentration curves for the species present in the reaction of **M2α-I** with

*cis*-[$PdCl_2(DMF)_2$]. Concentrations are given as the percentages of the initial **M2α-I** concentration.

A comparison of the results obtained via the UV-Vis and NMR time-resolved experiments on the **L2** and **M2α-I** systems reveals that for the second metalation step of the **L2** plus *cis*-[$PdCl_2(DMF)_2$] system, the values obtained for the second order rate constants are in extraordinary agreement (0.039 $M^{-1}$ $s^{-1}$ versus 0.040 $M^{-1}$ $s^{-1}$), which reinforces the idea that the β path is expected to be of minor importance due to a very low $K_3$ value. For the first metalation step, only the order of magnitude is in agreement (0.39 $M^{-1}$ $s^{-1}$ versus 1.0 $M^{-1}$ $s^{-1}$), a much more realistic results taking into account the large methodological differences used.

Even so, the difference for the latter can be associated very easily with the very high value of $k_{1\alpha}/k_{-1\alpha}$ obtained from the NMR measurements. This value (ca. 700-800 $M^{-1}$) should lead to the presence of an, unobserved, saturation behavior in the plots in Figures 3 and S7-S8. The difference can be associated to a very low, underestimated, value obtained for $k_{-1\alpha}$ dues to limitations of the NMR technique at very short times and low concentration of the **A2α-I** species (see Figure 6).

## CONCLUSIONS

We have conducted a comprehensive kinetico-mechanistic study of cyclopalladation reactions involving activation of azobenzene C–H bonds by *cis*-[$PdCl_2(DMF)_2$] in DMF, both on free ligands and on their already monopalladated derivatives. All reactions have been monitored by time-resolved NMR and UV-Vis spectroscopies at different palladium precursor concentrations, temperatures and pressures. The concentration profiles obtained by NMR monitoring, enabled a direct insight into the reactivity and nature of observed and putative intermediates, most of which have also been isolated and structurally characterized.

NMR results confirmed that the dipalladation of asymmetrically substituted azobenzenes is a multistep process involving two concurrent reaction paths. These involve an inverse sequential order for the C–H bond activation at the two possible cyclopalladation sites of the azo-derivative. A kinetic model, with a minimum number of fitting parameters has been found capable to explain the concentration-time profiles of the different reaction species. Very satisfactory results were obtained for some of the systems studied, providing a precise view of the reaction dynamics in solution. From the kinetic parameters obtained, one of the reaction paths is found to be dominant, a result also featured by the known computational study of the full process. The successful application of the kinetic model also supports the hypothesis that *bis*-palladium coordination compounds do not participate in azobenzene C–H bond activation at an appreciable extent.

Although less specific on the nature of the both reacting species and intermediates, UV-Vis monitoring has been successfully applied for the interpretation of the global kinetic model. Furthermore, the complete agreement of the data necessitates consideration of the two parallel paths resolved by NMR spectroscopy, despite one being dominant. The values of the thermal and pressure activation parameters, obtained at different temperatures and pressures, provided additional support for the electrophilic substitution mechanism operating in these cyclopalladation reactions. These values are consistent with a highly ordered and compressed transition state in which the basic DMF ligand participates in the proton abstraction producing an anionic species that quickly exchanges one of the two remaining chloride ligands by a new DMF ligand from the solvent

The results obtained represent an important contribution with a remarkable synergy between diverse but complementary techniques. This complete image of the full process will allow the better design and preparation of new cyclopalladated complexes in the Pd-catalyzed reactions of substrates having multiple C–H bonds available for functionalization.

## EXPERIMENTAL SECTION

**General Methods.** All chemicals and solvents were of reagent grade and used without additional purifications. NMR spectra of $CD_3CN$, DMF-$d_7$, and/or DMSO-$d_6$ solutions were recorded on Bruker AV-600, AV-400 and, AV-300 spectrometers at 25 °C. IR spectra were recorded on a Perkin-Elmer Spectrum Two spectrometer. CHN analyses were carried out with a Perkin-Elmer Series II 2400 CHNS/O analyzer. PXRD data were obtained by using Ni-filtered Cu$K_\alpha$ radiation on a PANalytical Aeris X-ray diffractometer. Single crystals structures of compounds **A1α-I, A3α-I** and **M1α-I**, **D1-I**, were isolated from standing MeCN and DMF solutions, respectively, and were measured on an Oxford Diffraction Xcalibur Nova R (microfocus Cu tube) at 20 °C.

**Kinetic Measurements**. The reactions of azobenzenes and their monopalladated compounds with *cis*-[$PdCl_2(DMF)_2$] precursor were monitored by time-resolved $^1$H NMR spectroscopy in DMF-$d_7$ solutions on a Bruker AV-400 spectrometer at 25 °C. Solutions for the kinetic runs were prepared by addition of 50 µL of a solution 6.04 ×$10^{-2}$ M in DMF-$d_7$ of the precursor to 500 µL of a solution of the ligand, or the monopalladated compound, (ca. 5.5 ×$10^{-4}$ M in DMF- $d_7$) in a NMR tube. After the addition of the *cis*-[$PdCl_2(DMF)_2$] solution, spectra were acquired at diverse time intervals, depending on the reaction rate. The kinetic traces of the species showing well resolved signals and good signal-to-noise ratio were fit with the Dynafit software.[16]

The same reactions were also followed by UV-Vis time-resolved spectroscopy at variable palladium precursor concentrations, temperatures and pressures. The variable temperature kinetic experiments at atmospheric pressure were monitored in the full 350-780 nm range on a Cary 50 UV–Vis spectrophotometer equipped with a thermostatted multicell transport (±0.1 ºC) and under pseudo-first-order conditions (palladium in at least 20-fold molar excess). The solutions were prepared by mixing the necessary volumes of a DMF solution of ligand, or monopalladated compound, with a DMF solution of *cis*-[$PdCl_2(DMF)_2$] in a 1 cm UV-Vis cuvette, the final volume was achieved by adding DMF. For the reactions carried out at varying pressure, the same sample preparation procedure was followed. The previously described pillbox cell and pressurizing system were used, and the final treatment of data was the same as described before.[4e] For these measurements, and given the excellent linearity observed for the $k_{obs}$ versus [Pd] plots

(see Figures 3 and S6-S7), the values of the second order rate constants were derived from a single $k_{obs}$/[Pd]) ratio at a given palladium precursor concentration (as done for some other very well-behaved systems).[18] The calculation of the observed rate constants from the absorbance *versus* time monitoring of reactions was carried out using the SPECFIT software.[19] All post-run fittings were carried out using standard software. In general, the errors for the rate constants derived were within the 5 % margin.

**Synthesis of Compounds**. The coordination complexes (**A1α-I**, **A2α-I**, **A3α-I** and **A5-III**) and monopalladated derivatives (**M1α-I**, **M2α-I**, **M3α-I**, **M4α-II**) were prepared in MeCN and DMF solution, respectively, by using the procedures recently developed for **A2α-I** and **M2α-I**.[8] Reaction of **L4** with $PdCl_2$ in MeCN afforded the mixture of **A4α-I** and **A4α-II** structures. Monopalladated complex **M5-II** was prepared in methanol according to the previously reported procedure.[8b]

*cis*-[$PdCl_2(DMF)_2$] was prepared by exposing solid $PdCl_2$ (60 mg, 0.34 mmol) to DMF vapor at room temperature for 72 h. Yield: quantitative. Found: C 21.90, H 4.66, N 8.88; Calcd. for $C_6H_{14}Cl_2N_2O_2Pd$: C 22.28, H 4.36, N 8.66.

[$PdCl_2(C_6H_5N{=}NC_6H_4NMe_2)$MeCN]·MeCN, **A1α-I** structure. A mixture of $PdCl_2$ (70 mg, 0.39 mmol) and **L1** (89 mg, 0.39 mmol) was stirred in MeCN for 30 h. The product was filtered off and dried under vacuum. Yield: 76%. Found: C 44.52, H 4.61, N 14.18; Calc. for $C_{18}H_{21}Cl_2N_5Pd$: C 44.60, H 4.37, N 14.45. $^1$H NMR (MeCN-$d_3$, $\delta$ / ppm, $J$ / Hz): 9.59 d (H-2,6, $^3J$(HH)=9.4), 7.09 d (H-3,5, $^3J$(HH)=9.5), 8.58 d (H-8,12, $^3J$(HH)=7.5), 7.50 t (H-9,11, $^3J$(HH)=7.9), 7.50 t (H-10, $^3J$(HH)=7.2), 3.27 s ($NMe_2$).

[$PdCl_2(IC_6H_4N{=}NC_6H_4NMe_2)$MeCN], **A3α-I** structure. A mixture of $PdCl_2$ (70 mg, 0.39 mmol) and **L3** (138 mg, 0.39 mmol) was stirred in MeCN for 30 h. The product was filtered off and dried under vacuum. Yield: 88%. Found: C 33.96, H 2.88, N 10.19; Calc. for $C_{16}H_{17}Cl_2IN_4Pd$: C 33.74, H 3.01, N 9.84. $^1$H NMR (MeCN-$d_3$, $\delta$ / ppm, $J$ / Hz): 9.60 d (H-2,6, $^3J$(HH)=9.3), 7.09 d (H-3,5, $^3J$(HH)=9.5), 8.37 d (H-8,12, $^3J$(HH)=8.5), 7.90 d (H-9,11, $^3J$(HH)=8.5), 3.28 s ($NMe_2$).

[$PdCl_2(C_6H_4N{=}NC_6H_5)_2$], **A5-III**. A mixture of $PdCl_2$ (50 mg, 0.28 mmol) and **L5** (102 mg, 0.56 mmol) was stirred in MeCN for 30 h. The product was filtered off, washed with diethyl ether and dried under vacuum. Yield: 48%. Found: C 52.81, H 3.97, N 10.13; Calc. for $C_{24}H_{20}Cl_2N_4Pd$: C 53.21, H 3.72, N 10.34. $^1$H NMR (DMF-$d_7$, $\delta$ / ppm, $J$ / Hz): 8.43 d (H-2,6, $^3J$(HH)=7.5), 7.93-7.99 m (H-3,4, 5), 8.34 d (H-8,12, $^3J$(HH)=8.6), 7.67 t (H-9,11, $^3J$(HH)=7.7), 7.78 t (H-10, $^3J$(HH)=7.4).

[$PdCl(C_6H_5N{=}NC_6H_3NMe_2)$(DMF)], **M1α-I**. Complex **A1α-I** (100 mg, 0.21 mmol) was stirred in DMF at room temperature for ten days. The product was filtered off and dried under vacuum. Yield 48 %. Found: C 46.86, H 4.95, N 12.55; Calc. for $C_{17}H_{21}ClN_4OPd$: C 46.48, H 4.82, N 12.76. $^1$H NMR (DMSO-$d_6$, $\delta$ / ppm, $J$ / Hz): 7.02 s, br (H-3), 6.58 d, br (H-5, $^3J$(HH)= 8.4), 7.62 d (H-6, $^3J$(HH)=7.6), 7.62 d (H-8, 12, $^3J$(HH)=7.6), 7.35 t (H-10, $^3J$(HH)=7.1), 7.42 t (H-9, 11, $^3J$(HH)=7.4), 3.13 s ($NMe_2$).

[$PdCl(C_6H_4IN{=}NC_6H_3NMe_2)$(DMF)], **M3α-I**. Complex **A3α-I** (100 mg, 0.18 mmol) was stirred in DMF at room temperature for seven days. The product was filtered off and dried under vacuum. Yield 67 %. Found: C 35.82, H 3.94, N 10.25; Calc. for $C_{17}H_{20}ClIN_4OPd$: C 36.13, H 3.57, N 9.91. $^1$H NMR (DMSO-$d_6$, $\delta$ / ppm, $J$ / Hz): 7.00 s, br (H-3), 6.59 d, br (H-5, $^3J$(HH)= 8.6), 7.62 d, br (H-6, $^3J$(HH)=8.5), 7.45 d (H-8, 12, $^3J$(HH)=8.4), 7.76 d (H-9, 11, $^3J$(HH)=8.6), 3.14 s ($NMe_2$).

[$Pd(\mu\text{-}Cl)(C_6H_4NO_2N{=}NC_6H_3NMe_2)]_2$, **M4α-II**. The mixture of complexes **A4α-I** and **A4α-II** (100 mg) was stirred in DMF at room temperature for seven days. The product was filtered off and dried under vacuum. Yield 51 %. Found: C 40.52, H 3.44, N 13.28; Calc. for $C_{28}H_{26}Cl_2N_8O_4Pd_2$: C 40.90, H 3.19, N 13.63. $^1$H NMR (DMSO-$d_6$, $\delta$ / ppm, $J$ / Hz): 7.09 s, br (H-3), 6.69 d, br (H-5, $^3J$(HH)= 8.3), 7.69 d, br (H-6, $^3J$(HH)=8.5), 7.90 d (H-8, 12, $^3J$(HH)=8.4), 8.26 d (H-9, 11, $^3J$(HH)=8.7), 3.20 s ($NMe_2$).

[{$PdCl(DMF)\}_2(\mu\text{-}C_6H_4N{=}NC_6H_3NMe_2)$], **D1-I**. A mixture of **M1α-I** (100 mg, 0.23 mmol) and *trans*-[$PdCl_2(MeCN)_2$] (118 mg, 0.46 mmol) was stirred in DMF for seven days at room temperature. The product was filtered off and dried under vacuum. Yield 75%. Found: C 36.44, H 4.42, N 10.38; Calcd. for $C_{20}H_{27}Cl_2N_5O_2Pd_2$: C 36.77, H 4.17, N 10.72. $^1$H NMR (DMSO-$d_6$, $\delta$ / ppm, $J$ / Hz): 7.23 s (H-3), 6.63 d (H-5, $^3J$(HH)= 9.6), 8.51 d (H-6, $^3J$(HH)=9.6), 7.68 d (H-9, $^3J$(HH)=7.7), 6.88 t (H-10, $^3J$(HH)=7.6), 7.05 t (H-11, $^3J$(HH)=7.6), 8.29 d (H-12, $^3J$(HH)=8.2), 3.19 s ($NMe_2$).

[{$PdCl(DMF)\}_2(\mu\text{-}C_6H_3ClN{=}NC_6H_3NMe_2)$], **D2-I**. A mixture of **M2α-I** (100 mg, 0.21 mmol) and *trans*-[$PdCl_2(MeCN)_2$] (109 mg, 0.42 mmol) was stirred in DMF for seven days at room temperature. The product was filtered off and dried under vacuum. Yield 83%. Found: C 34.55, H 3.36, N 9.95; Calcd. for $C_{20}H_{26}Cl_3N_5O_2Pd_2$: C 34.93, H 3.81, N 10.18. $^1$H NMR (DMSO-$d_6$, $\delta$ / ppm, $J$ / Hz): 7.23 s (H-3), 6.64 d (H-5, $^3J$(HH)=9.4 Hz), 8.49 d (H-6, $^3J$(HH)=9.3 Hz), 7.63 s (H-9), 7.13 d (H-11, $^3J$(HH)=8.7 Hz), 8.28 d (H-12, $^3J$(HH)=8.7 Hz), 3.20 s ($NMe_2$).

[{$PdCl(DMF\}_2$ ($\mu\text{-}C_6H_3IN{=}NC_6H_3NMe_2$)], **D3-I**. A mixture of **M3α-I** (100 mg, 0.18 mmol) and *trans*-[$PdCl_2(MeCN)_2$] (91 mg, 0.35 mmol) was stirred in DMF for seven days at room temperature. The product was filtered off and dried under vacuum. Yield 73%. Found: C 31.18, H 3.01, N 9.30.; Calcd. for $C_{20}H_{26}Cl_2IN_5O_2Pd_2$: C 30.83, H 3.36, N 8.99. $^1$H NMR (DMSO-$d_6$, $\delta$ / ppm, $J$ / Hz) 7.22 s (H-3), 6.65 d (H-5, $^3J$(HH)=9.8), 8.49 d (H-6, $^3J$(HH)=9.4), 7.99 s (H-9), 7.44 d (H-11, $^3J$(HH)=8.4), 8.04 d (H-12, $^3J$(HH)=8.3), 3.19 s ($NMe_2$).

[{$PdCl(DMF)\}_2(\mu\text{-}C_6H_3NO_2N{=}NC_6H_3NMe_2)$], **D4-I**. A mixture of **M4α-II** (100 mg, 0.12 mmol) and *trans*-[$PdCl_2(MeCN)_2$] (123 mg, 0.48 mmol) was stirred in DMF for seven days at room temperature. The product was filtered off and dried under vacuum. Yield 75%. Found: C 34.77, H 3.41, N 11.88. Calcd. for $C_{20}H_{26}Cl_2N_6O_4Pd_2$: C 34.40, H 3.75, N 12.04. $^1$H NMR (DMSO-$d_6$, $\delta$ / ppm, $J$ / Hz): 7.30 s (H-3), 6.80 d (H-5, $^3J$(HH)=9.1 Hz), 8.35 d (H-6, $^3J$(HH)=9.0 Hz), 8.43 s (H-9), 7.94 d (H-11, $^3J$(HH)=9.2 Hz), 8.59 d (H-12, $^3J$(HH)=9.2 Hz), 3.28 s ($NMe_2$).

[{$PdCl(DMF)\}_2(\mu\text{-}C_6H_4N{=}NC_6H_4)$], **D5-I**. A mixture of **M5-II** (80 mg, 0.12 mmol) and *trans*-[$PdCl_2(MeCN)_2$] (128 mg, 0.49 mmol) was stirred in DMF for 14 days at room temperature. The product was filtered off and dried under vacuum. Yield 73%. Found: C 35.07, H 3.26, N 9.39.; Calcd. for $C_{18}H_{22}Cl_2N_4O_2Pd_2$: C 35.43, H 3.63, N 9.18. $^1$H NMR (DMSO-$d_6$, $\delta$ / ppm, $J$ / Hz): 7.87 d (H-3, 9, $^3J$(HH)=7.2 Hz), 7.18 t (H-4, 10, $^3J$(HH)=7.2 Hz), 7.14 t (H-5, 11, $^3J$(HH)=7.23 Hz), 8.75 d, br (H-6, 12, $^3J$(HH)=6.9 Hz).

## ASSOCIATED CONTENT

### Supporting Information

The Supporting Information is available free of charge on the ACS Publications website at DOI:

Additional spectra, PXRD, kinetic data and computational details including DFT geometries and their energies are given. (PDF)

### Accession Codes

CCDC 1994905, 1995310-1995313 contain the supplementary crystallographic data for this paper. These data can be obtained free of charge via www.ccdc.cam.ac.uk/data_request/cif, or by emailing da-

ta_request@ccdc.cam.ac.uk, or by contacting The Cambridge Crystallographic Data Center, 12 Union Road, Cambridge CB2 1EZ, UK; fax: +44 1223 336033.

## AUTHOR INFORMATION

### Corresponding Author

EMAIL ADDRESSES: curic@irb.hr, dbabic@irb.hr, abudimir@pharma.hr, manel.martinez@qi.ub.edu

### Notes

‡ These authors contributed equally. The authors declare no competing financial interests.

## ACKNOWLEDGMENT

This work has been supported by Croatian Science Foundation under project number IP-2019-04-9951 and by the Spanish Ministerio de Ciencia e Innovación under project PID2019-107006GB-C21. Computations were done on the Isabella cluster at SRCE, Zagreb.

## REFERENCES

(1) (a) Dehand, J.; Pffefer,M. Cyclometallated Compounds. *Coord. Chem. Rev.* **1976**, *18*, 327-352. http://dx.doi.org/10.1016/S0010-8545(00)80431-2. (b) Omae, I. Intramolecular five-membered ring compounds and their applications. *Coord. Chem. Rev.* **2004**, *248*, 995-1023. https://doi.org/10.1016/j.ccr.2004.05.011. (c) Albrecht, M. Cyclometalation Using d-Block Transition Metals: Fundamental Aspects and Recent Trends. *Chem. Rev.* **2010**, *110*, 576-623. https://doi.org/10.1021/cr900279a. (d) Dupont, J.; Consorti, C. S.; Spencer, J. The Potential of Palladacycles: More than Just Precatalysts. *Chem. Rev.* 2005, *105*, 2527-2572. https://doi.org/10.1021/cr030681r. (e) *Palladacycles: Synthesis, Characterization and Applications* (Eds. Dupont, J.; Pfeffer, M.), Wiley-VCH, Weinheim, **2008**. (f) Ghedini, M.; Aiello, I.; Crispini, A.; Golemme, A.; La Deda, M.; Pucci, D. Azobenzenes and Heteroaromatic Nitrogen Cyclopalladated Complexes for Advanced Applications. *Coord. Chem. Rev.* **2006**, *290*, 1373-1390. https://doi.org/10.1016/j.ccr.2005.12.011. (g) Wakatsuki, Y.; Yamazaki, H.; Grutsch, P. A.; Santhanam, M.; Kutal, C. Study of Intramolecular Sensitization and Other Excited-State Pathways in Orthometalated Azobenzene Complexes of Palladium(II). *J. Am. Chem. Soc.* **1985**, *107*, 8153-8159. https://doi.org/10.1021/om9609574.

(2) (a) Ryabov, A. D. Cyclopalladated Complexes in Organic Synthesis. *Synthesis* **1985**, 233-252. https://doi.org/10.1055/s-1985-31169 3. (b) McNally, A.; Haffemayer, B.; Collins, B. S. L.; Gaunt, M. J. Palladium-Catalysed C–H Activation of Aliphatic Amines to Give Strained Nitrogen Heterocycles. *Nature*, **2014**, *510*, 129-133. https://doi.org/10.1038/nature13389. (c) Yamaguchi, J.; Yamaguchi, A. D.; Itami, K. C–H Bond Functionalization: Emerging Synthetic Tools for Natural Products and Pharmaceuticals. *Angew. Chem. Int. Ed*. **2012**, *51*, 8960-9009. https://doi.org/10.1002/anie.201201666. (d) Ackermann, L. Carboxylate-Assisted Transition-Metal-Catalyzed C-H Bond Functionalizations: Mechanism and Scope. *Chem. Rev*. **2011**, *111*, 1315-1345. https://doi.org/10.1021/cr100412j. (e) Godula, K.; Sames, D. C-H Bond Functionalization in Complex Organic Synthesis. *Science*, **2006**, *312*, 67-62. https://doi.org/10.1126/science.1114731.

(f) Lyons, T; W. Sanford, M. S. Palladium-Catalyzed Ligand-Directed C–H Functionalization Reactions. *Chem, Rev*. **2010**, *110*, 1147-1169. https://doi.org/10.1021/cr900184e.

(3) (a) Granell, J.; Martinez M. Kinetico-mechanistic studies of cyclometalating C–H bond activation reactions on Pd(II) and Rh(II) centres: The importance of non-innocent acidic solvents in the process. *Dalton Trans.* **2012**, *41*, 11243-11258. https://doi.org/10.1039/c2dt30866e. (b) Laga, E.; Garcia-Montero, A.; Sayago, F. J.; Soler, T.; Moncho, C.; Cativiela, C.; Martinez, M.; Urriolabeitia, E. P. Cyclopalladation and Reactivity of Amino Esters through C–H Bond Activation: Experimental, Kinetic, and Density Functional Theory Mechanistic Studies. *Chem. Eur. J.* **2013**, *19*, 17398-17412. https://doi.org/10.1002/chem.201302693. (c) Roiban, G.D.; Serrano, E.; Soler, T.; Aullón, G.; Grosu, I.; Cativiela, C.; Martinez, M.; Urriolabeitia, E. P. Regioselective Orthopalladation of (Z)-2-Aryl-4-Arylidene-5(4H)-Oxazolones: Scope, Kinetico-Mechanistic, and Density Functional Theory Studies of the C–H Bond Activation. *Inorg. Chem*. **2011**, *50*, 8132-8143. https://doi.org/10.1021/ic200564d. (d) Ryabov, A. D.; Sakodinskaya, I. K.; Yatsimirski, A. Kinetics and Mechanism of *Ortho*-Palladation of Ring-Substituted *N,N*-dimethylbenzylAmines K. *J. Chem. Soc. Dalton Trans*. **1985**, 2629-2638. https://doi.org/10.1039/DT9850002629. (e) Yagyu, T.; Aizawa, S.; Funahashi, S. Mechanistic Studies on Cyclopalladation of the Solvated Palladium(II) Complexes with *N*-Benzyl Triamine Ligands in Various Solvents. Crystal Structures of $[Pd(Sol)(Bn_2Medptn)](BF_4)_2$ (Sol = Acetonitrile and *N,N*-Dimethylformamide; $Bn_2Medptn$ = *N,N′* -Dibenzyl-4-methyl-4-azaheptane-1,7-diamine) and $[Pd(H_{-1}Bn_2Medptn\text{-}C,N,N',N'')]CF_3SO_3$. *Bull. Chem. Soc. Jpn*. **1998**, *71*, 619-629. https://doi.org/10.1246/bcsj.71.619. (f) Yagyu, T.; Iwatsuki, S.; Aizawa, S.; Funahashi, S. Electronic Effect of Substituents on Cyclopalladation of the Solvated Palladium(II) Complexes with *N*-Benzyl Triamine $[Pd(Sol)\{(4\text{-}XC_6H_4CH_2)NH(CH_2)_3NR(CH_2)_3NH_2\}]^{2+}$(Sol = Solvent; R = Ph, H, and Me; X = H, Et, Me, MeO, Cl, and $NO_2$). *Bull. Chem. Soc. Jpn*. **1998**, *71*, 1857-1862. https://doi.org/10.1246/bcsj.71.1857. (g) Gomez, M.; Granell, J.; Martinez, M. *Eur. J. Inorg. Chem*. **2000**, 217-224. https://doi.org/10.1002/(SICI)1099-0682(200001)2000:1<217::AID-EJIC217>3.0.CO;2-Q.

(4) (a) Babić, D.; Ćurić, M.; Smith, D. M. Computational Study of the Cyclopalladation Mechanism of Azobenzene with $PdCl_2$ in *N,N*-Dimethylformamide. *J. Organomet. Chem*. **2011**, *696*, 661-669. https://doi.org/10.1016/j.jorganchem.2010.09.038. (b) Juribašić, M.; Budimir, A.; Kazazić, S.; Ćurić, M. Dicyclopalladated Complexes of Asymmetrically Substituted Azobenzenes: Synthesis, Kinetics and Mechanisms. *Inorg. Chem*. **2013**, 52, 12749-12757. https://pubs.acs.org/doi/10.1021/ic402017v. (d) Font, H.; Font-Bardia, M.; Gómez, K.; González, G.; Granell, J.; Macho, I.; Martínez, M. A kinetico-mechanistic study on the C–H bond activation of primary benzylamines; cooperative and solid-state cyclopalladation on dimeric complexes. *Dalton Trans.* **2014**, 13525–135236. https://doi.org/10.1039/C4DT01463D. (e) Gomez, M.; Granell, J.; Martinez, M. Variable-temperature and-pressure kinetics and mechanism of the cyclopalladation reaction of imines in aprotic solvent. *Organometallics*, **1997**, *16*, 2593-2546. https://doi.org/10.1021/om9610990e. (f) Favier, I.; Gomez, M.; Granell, J.; Martinez., M.; Font-Bardia, M.; Solans, X.; Font-Bardia, M. Kinetico–mechanistic studies of C–H bond activation on new Pd complexes containing *N,N′* -chelating ligands. *Dalton. Trans*. **2005**, 123-132. https://doi.org/10.1039/B415613G. (g) Aullón, G.; Chat, R.; Favier, I.; Font-Bardia, M.; Gomez, M.; Granell, J.; Martinez, M.; Solans, X. Cyclometallation of amino-imines on palladium complexes. The effect of the solvent on the experimental and calculated mechanism. *Dalton Trans*, **2009**, 8292-8300. https://doi.org/10.1039/B905134A.

(5) (a) Grimster, N. P.; Gauntlett, C.; Godfrey, C. R. A.; Gaunt, M. J. Palladium-Catalyzed Intermolecular Alkenylation of Indoles by Solvent-Controlled Regioselective C–H Function-

alization. *Angew. Chem., Int. Ed.* **2005**, *44*, 3125-3129. https://doi.org/10.1002/anie.200500468. (b) Ulery, H. E. A Novel Preparation of Amidinium Arsenesulfonates. *J. Org. Chem.* **1965**, *30*, 2464-2465. https://doi.org/10.1021/jo01018a510. (c) Mei, T. S.; Wang, X.; Yu, J. Q. Pd(II)-Catalyzed Amination of C–H Bonds Using Single-Electron or Two-electron Oxidants. *J. Am. Chem. Soc.* **2009**, *131*, 10806-10807. https://doi.org/10.1021/ja904709b. (d) Chiong, H. A.; Pham, Q. N.; Daugulis, O. Two Methods for Direct ortho-Arylation of Benzoic Acids. *J. Am. Chem. Soc.* **2007**, *129*, 9879-9884. [DOI] https://doi.org/10.1021/ja071845e. (e) Zaitsev, V. G.; Daugulis, O. Highly Regioselective Arylation of $sp^3$ C–H Bonds Catalyzed by Palladium Acetate. *J. Am. Chem. Soc.* **2005**, *127*, 13154-13155. https://doi.org/10.1021/ja054549f.

(6) (a) Mottillo, C.; Lu, Y.; Pham, M.-H.; Cliffe, M. J.; Do, T.-O.; Friščić, T. Mineral Neogenesis as an Inspiration for Mild, Solvent-Free Synthesis of Bulk Microporous Metal–Organic Frameworks from Metal (Zn, Co) Oxides. *Green Chem.* **2013**, *15*, 2121. https://doi.org/10.1039/C3GC40520F. (b) Cliffe, M. J.; Mottillo, C.; Bučar, D.-K.; Friščić, T. Accelerated Aging: a Low Energy, Solvent-Free Alternative to Solvothermal and Mechanochemical Synthesis of Metal–Organic Materials *Chem. Sci.* **2012**, *3*, 2495. https://doi.org/10.1039/C2SC20344H (c) Braga, D.; Giaffreda, S. L.; Grepioni, F.; Chierotti, M. R.; Gobetto, R.; Palladino, G.; Polito, M. Solvent Effect in a "Solvent Free" Reaction. *CrystEngComm.* **2007**, *9*, 879. https://doi.org/10.1039/B711983F (d) Monas, A.; Užarević, K.; Halasz, I.; Juribašić Kulcsár, M.; Ćurić, M. Vapour-Induced Solid-State C–H bond Activation for the Clean Synthesis of an Organopalladium Biothiol Sensor. *Chem. Commun.* **2016**, *52*, 12960-12963. https://doi.org/10.1039/C6CC06062E.

(7) (a) Donati, M.; Morelli, D.; Conti, F.; Ugo, R. Complessi dimetilammidici di alcuni metalli del grupo del platino, *Chim. Ind.* **1968**, 50, 231-235. (b) Wayland, B. B.; Schramm, R. F. Cationic and Neutral Chloride Complexes of Palladium(II) with the Nonaqueous Solvent Donors Acetonitrile, Dimethyl Sulfoxide, and a Series of Amides. Mixed Sulfur and Oxygen Coordination Sites in a Dimethyl Sulfoxide Complex, *Inorg. Chem.* **1969**, 8, 971-976. https://doi.org/10.1021/ic50074a050. (c) Gioria, J. M.; Susz, B. P. Etude des composés d'addition des acides de Lewis – XXXV. Note sur les composés d'addition entre amides et, respectivement, $PdCl_2$ et $PtCl_2$, *Helv. Chim. Acta* **1971**, 54, 2251-2256. https://doi.org/10.1002/hlca.19710540762.

(8) Bjelopetrović, A.; Lukin, S.; Halasz, I.; Užarević, K.; Đilović, I.; Barišić, D.; Budimir, A.; Juribašić Kulcsár, Ćurić, M. Mechanism of Mechanochemical C-H Bond Activation in an Azobenzene Substrate by Pd(II) Catalysts. *Chem. Eur. J.* **2018**, *24*, 10672. https://doi.org/10.1002/chem.201802403.

(9) Juribašić Kulcsár, M.; Halasz, I.; Babić, D.; Cinčić, D.; Plavec, J.; Ćurić, M. Aging and Ball-Milling as Low-Energy and Environmentally Friendly Methods for the Synthesis of Pd(II) Photosensitizers. *Organometallics*, **2014**, *33*, 1227-1234. https://doi.org/10.1021/om500008v.

(10) Khare, G. P.; Little, R. G.; Veal, J. T.; Doedens, R. J. Crystal and Molecular Structure of Dichlorobis(azobenzene)palladium(II), a Possible Intermediate in the Ortho Palladation of Azobenzene. *Inorg. Chem.* **1975**, *14*, 2475-2479. https://doi.org/10.1021/ic50152a037.

(11) Ćurić, M.; Tušek-Božić, Lj.; Vikić-Topić, D.; Scarcia, V.; Furlani, A.; Balzarini, J.; DeClercq, E. Palladium(II) Complexes of Dialkyl α-Anilinobenzylphosphonates. Synthesis, Characterization, and Cytostatic activity. *J. Inorg. Biochem.* **1996**, *63*, 125-142. https://doi.org/10.1016/0162-0134(95)00199-9.

(12) Roy, S.; Hartenbach, I.; Sarkar, B. Structures, Redox and Spectroscopic Properties of $Pd^{II}$ and $Pt^{II}$ Complexes Containing an Azo Functionality. *Eur. J. Inorg. Chem.* **2009**, 2553–2558. https://doi.org/10.1002/ejic.200900007.

(13) (a) Babić, D.; Ćurić, M.; Molčanov, K.; Ilc, G.; Plavec, J. Synthesis and Characterization of Dicyclopalladated Complexes of Azobenzene Derivatives by Experimental and Computational Methods. *Inorg. Chem.* **2008**, *47*, 10446-10454. https://doi.org/10.1021/ic8010234. (b) Ćurić, M.; Babić, D.; Višnjevac, A; Molčanov, K. Simple Route to the Doubly ortho-Palladated Azobenzenes: Building Blocks for Organometallic Polymers and Metallomesogens. *Inorg. Chem.* **2005**, *44*, 5975. https://doi.org/10.1021/ic050747w.

(14) Ryabov, A. D. Mechanisms of intramolecular activation of carbon-hydrogen bonds in transition-metal complexes. *Chem. Rev.* **1990**, *90*, 403-424. https://doi.org/10.1021/cr00100a004.

(15) (a) Espenson, J. H. Chemical Kinetics and Reaction Mechanisms, McGraw-Hill, New York, **1981**. (b) Tobe, M. L.; Burgess, J. Inorganic Reaction Mechanisms, Longman, New York, **1999**.

(16) (a) Kuzmič, P. Program DYNAFIT for the analysis of enzyme kinetic data: Application to HIV proteinase. *Anal. Biochem.* **1996,** *237*, 269-273. https://doi.org/10.1006/abio.1996.0238. (b) Kuzmič, P. DYNAFIT – a software package for enzymology. Methods Enzymol. **2009,** *467*, 247-280. https://doi.org/10.1016/S0076-6879(09)67010-5.

(17) Wakatsuki, Y.; Yamazaki, H.; Grutsch, P. A.; Santhanam, M.; Kutal, C. Study of intramolecular sensitization and other excited-state pathways in orthometalated azobenzene complexes of palladium(II). *J. Am. Chem. Soc.* **1985**, *107*, 8153-8159. https://doi.org/10.1021/om9609574.

(18) Bernhard, P. V.; Gonzálvez, M.V.; Martinez, M. Kinetico-mechanistic Study on the Oxidation of Biologically Active Iron(II) Bis(thiosemicarbazone) Complexes by Air. Importance of NH···$O_2$ Interactions as Established by Activation Volumes. *Inorg. Chem.* **2017**, *56*, 1428-14290. https://pubs.acs.org/doi/abs/10.1021/acs.inorgchem.7b02381.

(19) Binstead, R. A.; Züberbuhler A. D.; Jung, B. SPECFIT32. [3.0.34], Spectrum Software Associates, **2005**.

Table of Contents Synopsis

A kinetico-mechanistic study of the C–H bond activation in azobenzenes and their monopalladated derivatives with *cis*-[$PdCl_2(DMF)_2$] in DMF has been conducted by time-resolved NMR and UV-Vis spectroscopies at variable concentration, temperature and pressure. NMR spectra enabled detailed insight into the nature and reactivity of intermediates and confirmed that the dipalladation of 4,4′ -functionalized azobenzenes is a multistep process involving two reaction pathways

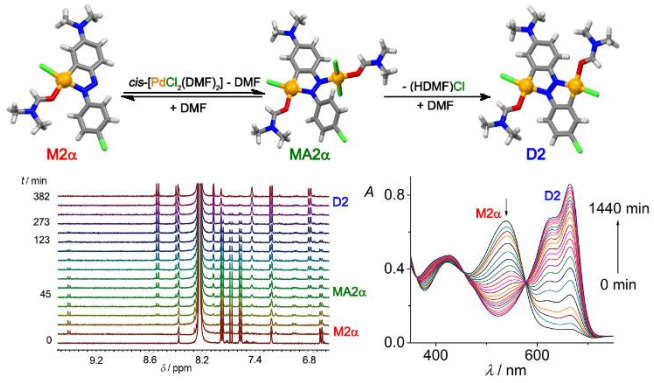
cis-[PdCl2(DMF)2] - DMF
+ DMF
- (HDMF)Cl
+ DMF
M2α
MA2α
D2
t / min
382
273
123
45
0
D2
MA2α
M2α
9.2
8.6
8.2
7.4
6.8
δ / ppm
A
0.8
0.4
0.0
M2α
D2
1440 min
0 min
400
600
λ / nm